Formation of Au–Carbon Nanoparticles by Laser Ablation under Pressurized CO_2

Mardiansyah Mardis [1], Wahyudiono[2], Noriharu Takada [2], Hideki Kanda[2], Motonobu Goto[2]*

[1] *Department of Chemical Engineering, Nagoya University, Nagoya, 464-8603, Japan*

[2] *Department of Materials Process Engineering, Nagoya University, Nagoya, 464-8603, Japan*

* *Corresponding Author. E-mail: goto.motonobu@material.nagoya-u.ac.jp (M. Goto), Tel: +81-52-789-3392, Fax: +81-52-789-3989*

Abstract

Pulsed laser ablation (PLA) is known to be a promising method for synthesizing metal nanoparticles. Here, Au–carbon nanoparticles were synthesized by PLA under pressurized carbon dioxide (CO_2). Au plate was ablated using a Nd: YAG laser with a wavelength of 532 nm and energy of 0.83 mJ in a high-pressure chamber. The experiments were performed at temperatures and pressures of 21-25°C and 7-15 MPa, corresponding to CO_2 densities of 0.75-0.89 g/cm^3, respectively. The synthesized products were collected on a silicon wafer and analyzed using field emission scanning electron microscopy (FE-SEM), transmission electron microscopy (TEM) and a scanning transmission electron microscopy (STEM) system equipped with energy dispersive X-ray spectroscopy (EDS). The results showed that the generated metal nanoparticles exhibited spherical and nanocluster structures. Au, C, and O were clearly found on the nanoparticle products.

Keywords:

Gold nanoparticles; Gold–carbon particles; Pressurized CO_2; Laser ablation

1. Introduction

Bare metal nanoparticles easily oxidize and degrade under ambient conditions, and thus, many researchers have attempted to develop ways to prevent these issues. Synthesizing metal–carbon (i.e., carbon-coated) particles is recognized as an excellent way to enhance the chemical stability of the inner metals from oxidation and to improve their stability in harsh environments, such as acidic or basic environments and high operating temperatures and/or pressures [1-3]. Moreover, metal–carbon nanoparticles may prevent the cores from agglomerating, and their biocompatibility enables using them for biomedical applications. In mechanical and electrochemical applications, metal–carbon nanoparticles may also exhibit improved thermal stability, wear resistance, and electrical conductivity [4].

Various techniques have been reported for synthesizing metal–carbon nanoparticles, such as arc discharge plasma, chemical vapor deposition (CVD), spray pyrolysis, and pulsed laser ablation (PLA). The simplest and most popular technique is the arc discharge plasma technique [5]. In this technique, two electrodes (carbon and metal electrodes) facing each other are connected to an electric power source to produce high-temperature plasma. The metal electrode enables producing the desired metal nanoparticles due to the high temperature of the plasma. The interaction between these metal nanoparticles with the carbon generated from the carbon electrode results in the formation of metal–carbon nanoparticles. Another simple technique is CVD, which may be easier to scale up for economically viable production. The process is conducted at temperatures of 600-1000°C and pressures of 40-100 Pa [6]. Similar to CVD, the spray pyrolysis technique is also performed at high temperatures (600-1000°C) [7,8]. The synthesized metal–carbon nanoparticles are produced by atomizing the reaction solution using a spray nozzle. This technique enables utilizing different types of precursors in the gas or liquid phase. In the PLA technique, a highly energetic laser beam interacts with a metal to disintegrate and vaporize the metal, forming a gaseous plasma containing atoms, molecules, ions, excited species, clusters, nanodroplets of melted material, etc., called the ablation plume. For metal–carbon nanoparticles, the metal target is generally immersed in a liquid medium. The metal–carbon nanoparticles can be synthesized due to the interactions between metal nanoparticles and the carbon in the reaction medium, which quickly quenches the laser ablation plume [9,10].

In this paper, metal–carbon nanoparticles were synthesized using the PLA technique under pressurized carbon dioxide (CO_2). Au plates were used as the source metal for the nanoparticles. As an abundant natural carbon source, CO_2 is relatively benign with regard to both environmental and health effects. CO_2 has also found widespread application in a variety of industries because it is relatively non-reactive, non-toxic, nonflammable, and readily attainable critical properties. Moreover, the density of pressurized CO_2 can be adjusted by tuning the pressure and temperature [11,12]. As a result, the heat and mass transfer rates of pressurized CO_2 are considerably higher than those of CO_2 at ambient condition, which is beneficial for generating metal–carbon nanoparticles by the PLA technique. Furthermore, employing CO_2 as the reaction medium has been shown to prevent contaminating the generated nanoparticles with impurities from the organic solvents usually used as a reaction medium [9,10]. This paper presents further insight from the previously reported gold nanoparticles synthesis via PLA in pressurized or supercritical CO_2 [11,13,14] since we conducted more comprehensive analysis. We demonstrate that the generated Au nanoparticles were not pristine Au nanoparticles as believed in earlier studies, but the composite of Au and C nanoparticles.

2. Materials and Methods

Figure 1 shows a schematic diagram of the laser ablation system used to generate nanoparticles under pressurized CO_2. Au plate, purchased from Nilaco Co., Japan, with dimensions of 10 × 10 mm and a thickness of 1 mm was used as the target material. A silicon wafer with a thickness of 1 mm and dimensions of 7 × 7 mm, also purchased from Nilaco Co, Japan, was employed as the collector for the generated particles. CO_2 (99.95%) was supplied from Sogo Co., Japan and used as the reaction medium.

A high-power Q-switched pulsed Nd: YAG laser (Spectra-Physics Quanta-Ray INDI-40-10), with a wavelength of 532 nm, pulse energy of 0.83 mJ, pulse rate of 10 Hz, and pulse duration of approximately 8 ns, was used to ablate the metal target, which was placed at the center of a high-pressure chamber constructed from SUS 316 stainless steel (110 mL in volume, 6.5 cm in diameter, AKICO, Japan), and the Nd:YAG laser was located approximately 1 m from the target. The laser beam was focalized by a 1-mm-diameter of apperture. The silicon wafer was placed beneath the Au target in order to collect the generated nanoparticles. Figure 1 also shows the positions of the metal plate and Si wafer inside high-pressure chamber. CO_2 was pressurized and pumped into the chamber using a high-performance liquid chromatography (HPLC) pump (PU-1586, Jasco Co., Japan). The chamber temperature was regulated with a temperature controller, and the pressure was controlled with a back-pressure regulator. The temperature and pressure ranges for the experiments were 21-25°C and 7-15 MPa corresponding to 0.75-0.89 g/cm^3 of CO_2 density, respectively. A thermocouple for monitoring the experimental temperature was inserted into the chamber. K-type thermocouples were also inserted into the chamber's walls to measure the radial temperature distribution. After the desired pressure and temperature were attained, PLA was performed for 15 min. After the CO_2 medium naturally evaporated, the particles deposited on the silicon wafer were collected and then characterized by field emission scanning electron microscopy (FE-SEM, Model JSM-6330F, JEOL, Japan). Particle size characterization was also performed using (scanning) transmission electron microscopy, (S)TEM, with a JEM-2100F HK model operating at 200 kV and equipped with CCD camera. (S)TEM samples were prepared by placing carbon grids below the target material in the same position as that of the Si wafer to collect the particles. In order to determine the products

elemental composition, scanning transmission electron microscopy with energy dispersive X-ray spectroscopy (STEM-EDS) (Model JEM-2100F HK, JEOL, Japan) was also performed.

3. Results and Discussion

In previous studies, when CO_2 was employed as the medium for generating metal–carbon nanoparticles, one of the important advantages that PLA in CO_2 exhibited over the conventional multistep chemical synthesis techniques was the absence of contaminants, which may come from the intermediate medium. Applying PLA directly to the metal target eliminates the need for chemical precursors and enables generating clean nanoparticles. Figure 2 shows FE-SEM and scanning TEM (STEM) images of Au nanoparticles generated by PLA under pressurized CO_2 with a density 0.75 g/cm^3. As discussed above, plasma, vapor, and nano/micro-sized molten metallic droplets could be generated as initial products when the pulsed laser beam was introduced to heat the metal target. These products then reacted with elements in the reaction medium to produce nanoparticles [9,10]. Consequently, the generated metal nanoparticles consisted of spherical and nanocluster structures. Employing highly compressed CO_2 as the medium enabled achieving large changes in density with small changes in temperature and/or pressure. Thus, pressurized CO_2 may lead to the formation of a colloidal medium. As a result, the generated Au nanoparticles were also mainly composed of spherical and nanocluster structures, as shown in Fig. 2. In the images, a network structure of smaller Au nanoclusters seems to surround larger Au nanoparticles. This arrangement may form due to the fast coagulation and quenching of the Au atoms in the dense CO_2 environment [13]. Saitow et al. [14] performed nanosecond PLA with an excitation wavelength of 532 nm in supercritical CO_2 to produce Au nanoparticles. Those Au nanoparticles exhibited two different morphologies: large nanospheres and nanonecklaces (nanoclusters). They reported that the nanonecklaces were a few tens of micrometers long, and the large Au nanospheres were 500 nm in diameter. Similar results were also reported by Machmudah et al. [13]. They performed PLA under pressurized CO_2 at pressures of 0.2-20 MPa and temperatures of 20-80°C, which generated spherical Au nanoparticles and a network structure of small Au nanoparticles.

When CO_2 is pressurized and heated above its critical point, CO_2 exhibits interesting properties such as a liquid-like density and gas-like viscosity, and the diffusion coefficients in these conditions are higher than those of liquids. When the temperature of CO_2 is lower than its critical temperature and more pressure is applied, CO_2 becomes denser. At these

conditions, CO_2 may have liquid-like properties, but no liquid forms. Similar to supercritical CO_2, the advantages of dense CO_2 as a reaction medium over other solvents are primarily due to its physicochemical properties. Dense CO_2 is an intermediate between a gas and a liquid, and its properties are easily adjustable by shifting the temperature and pressure [15]. Therefore, when PLA was applied in dense CO_2 as the medium, high-density plasmas were also generated [9]. Figure 3 shows FE-SEM and STEM images of Au nanoparticles generated by PLA under pressurized CO_2 with various CO_2 densities. It should be noted that no experiments were conducted with low-density CO_2 (less than 0.60 g/cm^3) in order to maintain liquid-like physical properties, which require densities of around 0.60-1.6 g/cm^3. The generated Au nanoparticles clearly exhibited nanosphere-like and nanocluster morphologies. Nanoparticles formed when the PLA was applied at CO_2 densities of 0.75 (Fig. 2) and 0.80 g/cm^3 (Fig. 3). As the CO_2 density increased (0.89 g/cm^3), the generated Au nanoparticles were also apparently composed of Au nanoclusters and the Au nanosphere-like structure. The Au nanosphere-like structure generated at 0.89 g/cm^3 in Fig. 3 appears smaller than those generated under other conditions. Similar to the generation of metal nanoparticles by PLA in aqueous media, the production of Au nanoparticles by PLA under high-density CO_2 was affected by several parameters such as laser fluence, irradiation time, excitation wavelength, pulse width, and the CO_2 phase [9,14,16]. Generally, the PLA plasma plume evolution in a confining liquid leads to cluster formation, nucleation, and crystals growth during the ablation process. Hence, the PLA plasma plume in high-density CO_2 will also rapidly quench in the confining liquid-like CO_2. As a result, the short quenching times of the PLA plasma plume enables restricting the size of the grown Au particles and producing Au nanoclusters [9]. Saitow et al. [14] performed PLA in supercritical CO_2. They showed that nanoparticles and nanoclusters could be produced and deposited since these products were not soluble in supercritical CO_2. They reported that the size of the generated nanosphere particles did not depend on the density of the CO_2 medium.

In addition, we measured the particle size distribution of the generated particles using the ImageJ program to analyze TEM images. Figure 4 shows typical TEM micrographs of generated Au particles in pressurized CO_2. Similar to the SEM images, the TEM images in Fig. 4(a), (b) and (c) indicate that the particles generated under each set of conditions are

spherical. These results are similar to those of a work previously reported on PLA in liquid CO_2 using a Nd: YAG laser with a laser energy of 2.46 mJ [16].

Au nanoparticles prepared by PLA in pressurized CO_2 were well dispersed and exhibited a broad size distribution, as shown in Fig. 4. At an identical laser power of 0.83 mJ, the average size of nanoparticles decreased from 16.0 to 8.9 nm with the density of CO_2 increasing from 0.75 to 0.89 g/cm^3. We note that some literatures report that nanoparticles synthesized in the pressurized liquid medium via PLA has smaller size with increasing medium pressure (or increasing density). For instance, the average size of ZnO nanoparticles synthesized in water [24,25] decreased from 50 - 100 nm at ambient condition down to below 20 nm at 31 MPa at constant temperature. Sn nanoparticles synthesized in pressurized CO_2 exhibits similar phenomenon [26]. Thus, it can be safely generalized that increasing the pressure of the medium has the effect to decrease the size of nanoparticles.

STEM-EDS was performed to analyze the presence of carbon on the generated nanoparticles. Several reports [9,16,21,22,23] have concluded that the PLA reaction medium and ablated matter can react during the formation of particles. However, the alloy nanoparticle formation mechanism during PLA and the process mechanisms are still not well understood. Figure 5 shows the STEM-EDS mapping of nanoparticles generated in CO_2 with various densities.

In order to understand the chemical composition of the generated Au nanoparticles, they were characterized using a STEM system equipped with EDS. This method distinguishes the characteristic X-rays emitted from the analyte by their energy levels. Since each element has a unique atomic structure, the atomic structure could be identified individually from one another. Hence, EDS analysis is a reliable way to investigate the sample using the interactions between electromagnetic radiation and matter.

Figure 5 shows STEM images and EDS patterns of the generated Au nanoparticles when PLA was applied at CO_2 densities of 0.70, 0.80 and 0.89 g/cm^3. The EDS spectrum clearly shows that the Au, C, and O were detected.

The spectroscopic analysis demonstrated that the generated particles were almost completely composed of Au under each set of conditions. The spectra clearly exhibit a high C peak due to the TEM grid, which contains considerable C. O was also detected by

spectroscopy, although the peak was not high compared to those of Au and C. However, particles generated under all conditions contained Au, C and O. As a reaction medium, CO_2 is well known to decompose into C and O during PLA [19,20], as evidenced in Fig. 5. Interestingly, Au, C, and O were uniformly distributed on the outermost surface, which could be attributed to the dissociation of the CO_2 reaction medium into CO molecules, C atoms, and O atoms during PLA. The CO_2 dissociation products may induce chain reaction with other CO_2 molecules. The possible phenomenon that occurred is the reactive C, CO and O collide with other CO_2 molecules or themselves to form a large hollow carbon nanostructure layer (i.e. "sp2 amorphous carbon") that covers the Au nanoparticles and nanoclusters [19]. The O atoms can oxidize the carbon nanostructure since O can still be covalently bound to the sp2 amorphous carbon type nanostructure. However, the EDS spectra indicate that there is only a trace amount of O on the nanostructures, indicating that only partial oxidation occurred. Therefore, C and O were both observed on the generated Au nanoclusters in this study.

Further, the corresponding selected area diffraction pattern of generated particles in each condition are shown in Fig. 6. The characteristic rings in polycrystalline diffraction pattern can be indexed to the {111}, {200}, {220}, and {311} planes for each condition, that expected from fcc Au [27]. These results are witnessed our previous explanation, that almost particles are formed by gold and only partial part of generated particles are formed by carbon.

4. Conclusions

Au nanoparticles with carbon were successfully synthesized using the PLA method under pressurized CO_2. The PLA was carried out at temperatures of 21-25°C with CO_2 densities of 0.75-0.89 g/cm^3 and an irradiation time 15 min. The generated nanoparticles were characterized using a STEM system equipped with EDS. SEM images exhibited generated metal nanoparticles with spherical and nanocluster morphologies. The network structure of smaller metal nanoclusters appears to surround the larger metal nanoparticles. According to STEM-EDS results, Au, C, and O were found to be uniformly distributed on the generated nanoclusters. Further, the average size of nanoparticles decreased from 16.0 to 8.9 nm with the density of CO_2 increasing from 0.75 to 0.89 g/cm^3. The results suggest that this method enables obtaining advanced nanostructured materials.

Acknowledgments

This work was supported by Grants-in-Aid for Scientific Research (No. 21246119 and No. 21110009) from the Ministry of Education, Culture, Sports, Science and Technology, Japan.

References

[1] Wang, S., Huang, X., He, Y. et al. (2012). Synthesis, Growth Mechanism and Thermal Stability of Copper Nanoparticles Encapsulated by Multi-layer Graphene. *Carbon*, 50: 2119-2125.

[2] Love, C.A., Cook, R.B., Harvey, T.J., Dearnley, P.A., Wood, R.J.K. (2013). Diamond Like Carbon Coatings for Potential Application in Biological Implants—A Review, *Tribology International*, 63: 141-150.

[3] Espinoza-Rivas, A.M., Pérez-Guzmán, M.A., Ortega-Amaya, R., Santoyo-Salazar, J., Gutiérrez-Lazos, C.D., Ortega-López, M. (2016). Synthesis and Magnetic Characterization of Graphite-Coated Iron Nanoparticles, *Journal of Nanotechnology*, 2016: 6.

[4] Sattler, Klaus D. ed. (2010). *Handbook of Nanophysics: Principles and Methods*, CRC Press, Taylor and Francis Group, LLC.

[5] Wei, Z.Q., Liu, L.G., Yang, H. et al. (2011). Characterization of Carbon Encapsulated Fe-nanoparticles Prepared by Confined Arc Plasma, *Transactions of Nonferrous Metal Society of China*. 21: 2026-2030.

[6] Sarno, M., Cirillo, C., Ciambelli, P. (2014). Selective Graphene Covering of Monodispersed Magnetic Nanoparticles, *Chemical Engineering Journal*. 246: 27-38.

[7] Jung, D.S., Park, S.B., Kang, Y.C. (2010). Design of Particles by Spray Pyrolysis and Recent Progress in its Application, *Korean Journal of Chemical Engineering*. 27: 1621-1645.

[8] Atkinson, J.D., Fortunato, M.E., Dastgheib, S.A. et al. (2011). Synthesis and Characterization of Iron-impregnated Porous Carbon Spheres Prepared by Ultrasonic Spray Pyrolysis. *Carbon*. 49: 587-598.

[9] Yang, G.W. (2007). Laser Ablation in Liquids: Applications in the Synthesis of Nanocrystals. *Progress in Materials Science*. 52: 648-698.

[10] Zeng, H., Du, X.W., Singh, S.C. et al. (2012). Nanomaterials via Laser Ablation/Irradiation in Liquid: A Review. *Advanced Functional Materials*. 22: 1333-1353.

[11] Machmudah, S., Wahyudiono, Kuwahara, T., Sasaki, M., Goto, M. (2011). Nano-structured Particles Production Using Pulsed Laser Ablation of Gold Plate in Supercritical CO_2. *Journal of Supercritical Fluids*. 60: 63-68.

[12] Machmudah, S., Sato, T., Wahyudiono, Sasaki, M., Goto, M. (2012). Silver Nanoparticles Generated by Pulsed Laser Ablation in Supercritical CO_2 Medium. *High Pressure Research*, 32: 60-66.

[13] Machmudah, S., Wahyudiono, Takada, N., Kanda H., Sasaki, K., Goto, M. (2013). Fabrication of Gold and Silver Nanoparticles with Pulsed Laser Ablation Under Pressurized CO_2, *Advances in Natural Sciences: Nanosciences and Nanotechnology*. 4: 045011-045018.

[14] Saitow, K., Yamamura, T., Minami T. (2008). Gold Nanospheres and Nanonecklaces Generated by Laser Ablation in Supercritical Fluid. *Journal of Physical Chemistry C*. 112: 18340-18349.

[15] Sanli, D., Bozbag, S.E., Erkey, C. (2012). Synthesis of Nanostructured Materials Using Supercritical CO_2: Part I. Physical Transformations. *Journal of Materials Science*. 47: 2995-3025.

[16] Mardis, M., Takada, N., Machmudah, S., Wahyudiono, Sasaki, K., Kanda H., Goto, M. (2016). Nickel Nanoparticles Generated by Pulsed Laser Ablation in Liquid CO_2. *Research on Chemical Intermediates*. 42: 4581-4590.

[17] Boutinguiza, M., Comesaña, R., Lusquiños, F., et al. (2015). Production of Silver Nanoparticles by Laser Ablation in Open Air. *Applied Surface Science*. 336: 108-111.

[18] Minaev, N.V., Arakcheev, V.G., Rybaltovskii, A.O., et al. (2015). Dynamics of Formation and Decay of Supercritical Fluid Silver Colloid under Pulse Laser Ablation Conditions. *Russian Journal of Physical Chemistry B*. 9: 1074-1081.

[19] Fukuda, T., Maekawa, T., Hasumura, T., et al. (2007). Dissociation of Carbon Dioxide and Creation of Carbon Particles and Films at Room Temperature. *New Journal of Physics*. 9: 321.

[20] Nakahara, S., Stauss, S., Kato, T. et al. (2011). Synthesis of Higher Diamondoids by Pulsed Laser Ablation Plasmas in Supercritical CO_2. *Journal of Applied Physics*. 109:

123304.

[21] Moslehirad, F., Majles Ara, M.H., Torkamany, M.J. (2013). Synthesis of composite Au/TiO_2 nanoparticles through pulsed laser ablation and study of their optical properties. *Laser Physics*. 23: 075601.

[22] Amendola, V., Scaramuzza, S., Carraro, F. et al. (2016). Formation of alloy nanoparticles by laser ablation of Au/Fe multilayer films in liquid environment. *Journal of Colloid and Interface Science*. 489: 18-27.

[23] Hajiesmaeilbaigi, F., Motamedi, A., Ruzbehni, M. (2009). Synthesis and Characterization of Composite Au/TiO_2 Nanoparticles by Laser Irradiation. *Laser Physics*. 20: 508-511.

[24] Kulinich, S., Kondo, T., Shimizu, T. et al. (2013) Pressure effect on ZnO nanoparticles prepared via laser ablation in water. *Journal of Applied Physics*. 113: 033509.

[25] Soliman, W., Takada, N., Koshizaki, N. et al. (2013). Structure and size control of ZnO nanoparticles by applying high pressure to ambient liquid in liquid-phase laser ablation. *Applied Physics A*. 10: 779

[26] Koizumi, M., Kulinich, S., Shimizu, Y. et al. (2013). Medium slow dynamics of ablated zone observed around the density fluctuation ridge of fluid medium. *Journal of Applied Physics*. 114: 214301.

[27] Lü, X., Song, Y., Zhu, A. et al. (2012). Synthesis of Gold Nanoparticles Using Cefopernazone as a Stabilizing Reagent and Its Application. *Int. J. Electrochem. Sci*. 7: 11236-11245.

FIGURE CAPTIONS

Figure 1. Schematic diagram of PLA under pressurized CO_2.

Figure 2. (a), (b) FE-SEM and (c), (d) STEM images of Au nanoparticles generated by PLA at density 0.75 g/cm^3 (7.3 MPa; 23.4°C).

Figure 3. FE-SEM (top) and STEM images (bottom) of Au nanoparticles generated by PLA at CO_2 densities of (a), (c) 0.80 g/cm^3 (9.1 MPa; 24.5°C) and (b), (d) 0.89 g/cm^3 (17.5 MPa; 25.1°C).

Figure 4. TEM images (top) and size distributions (bottom) of Au nanoparticles generated by PLA at CO_2 densities of (a), (d) 0.75 g/cm^3 (7.3 MPa; 23.4°C), (b), (e) 0.80 g/cm^3 (9.1 MPa; 24.5°C), and (c), (f) 0.89 g/cm^3 (17.5 MPa; 25.1°C).

Figure 5. EDS mappings of particles generated at CO_2 densities of (a) 0.75 g/cm^3, (b) 0.80 g/cm^3, and (c) 0.89 g/cm^3.

Figure 6**.** Electron diffraction pattern of particles generated at CO_2 densities of (a) 0.75 g/cm^3, (b) 0.80 g/cm^3, and (c) 0.89 g/cm^3.

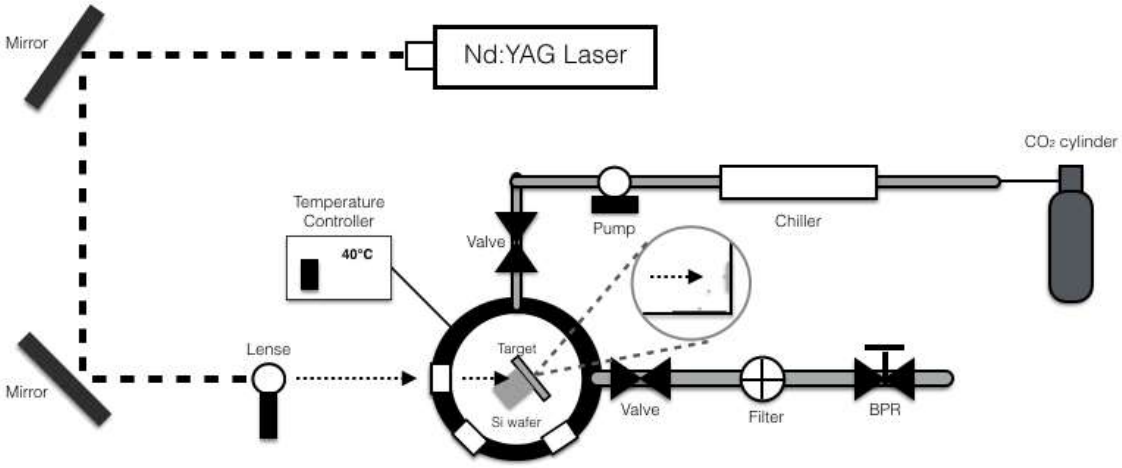

Figure 1. Schematic diagram of PLA under pressurized CO_2.

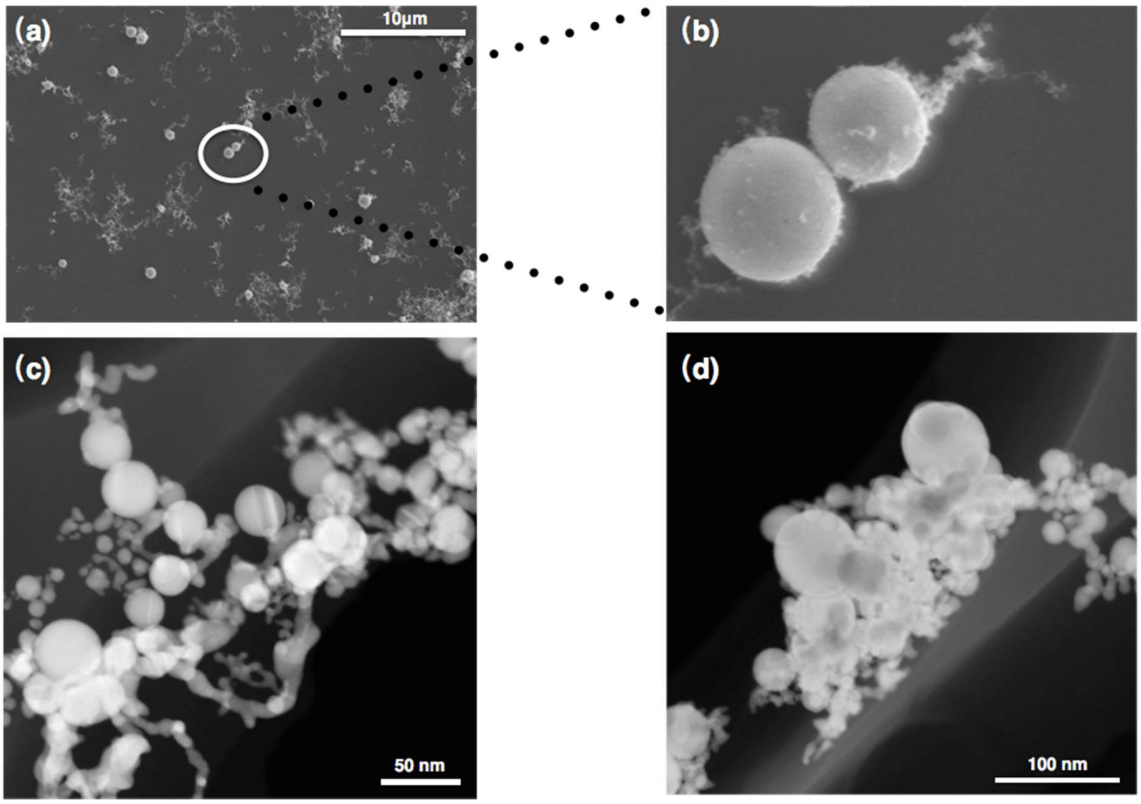

Figure 2. (a), (b) FE-SEM and (c), (d) STEM images of Au nanoparticles generated by PLA at density 0.75 g/cm^3 (7.3 MPa; 23.4°C).

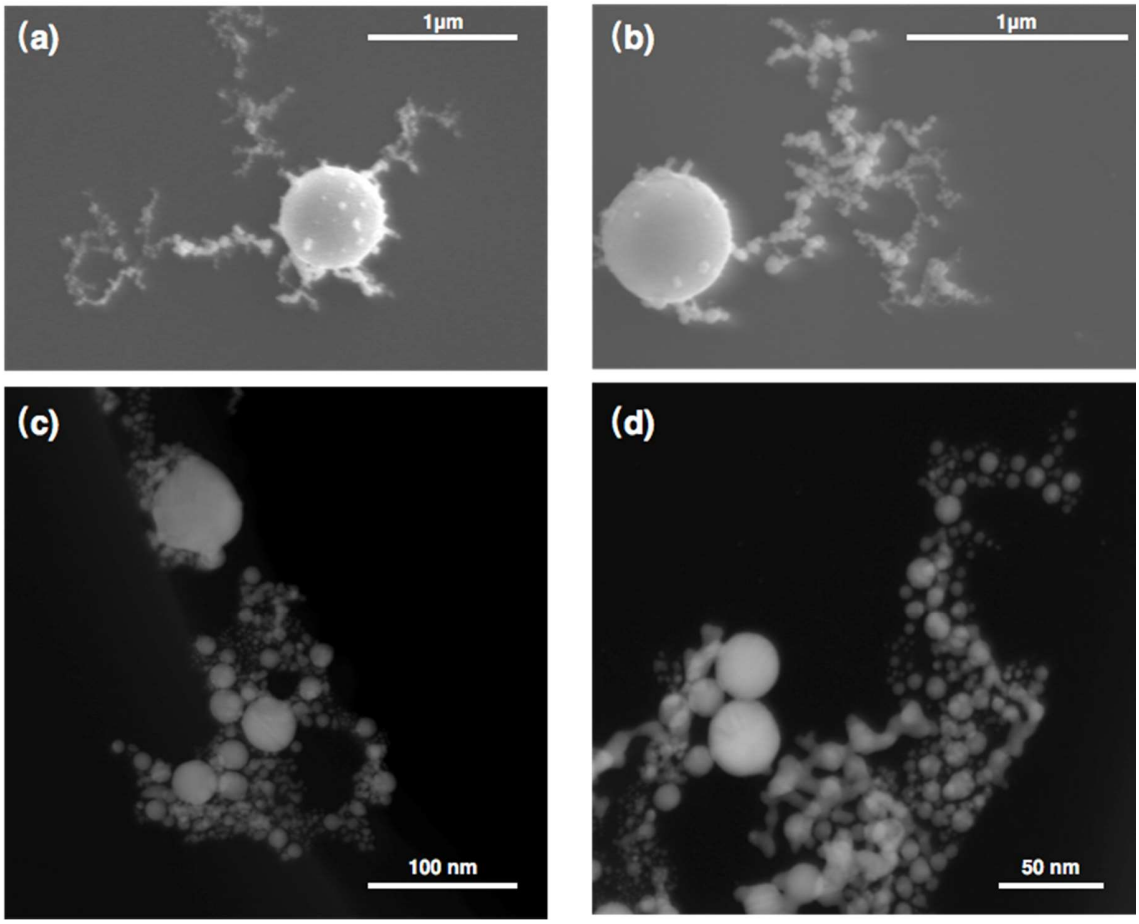

Figure 3. FE-SEM (top) and STEM images (bottom) of Au nanoparticles generated by PLA at CO_2 densities of (a), (c) 0.80 g/cm^3 (9.1 MPa; 24.5°C) and (b), (d) 0.89 g/cm^3 (17.5 MPa; 25.1°C).

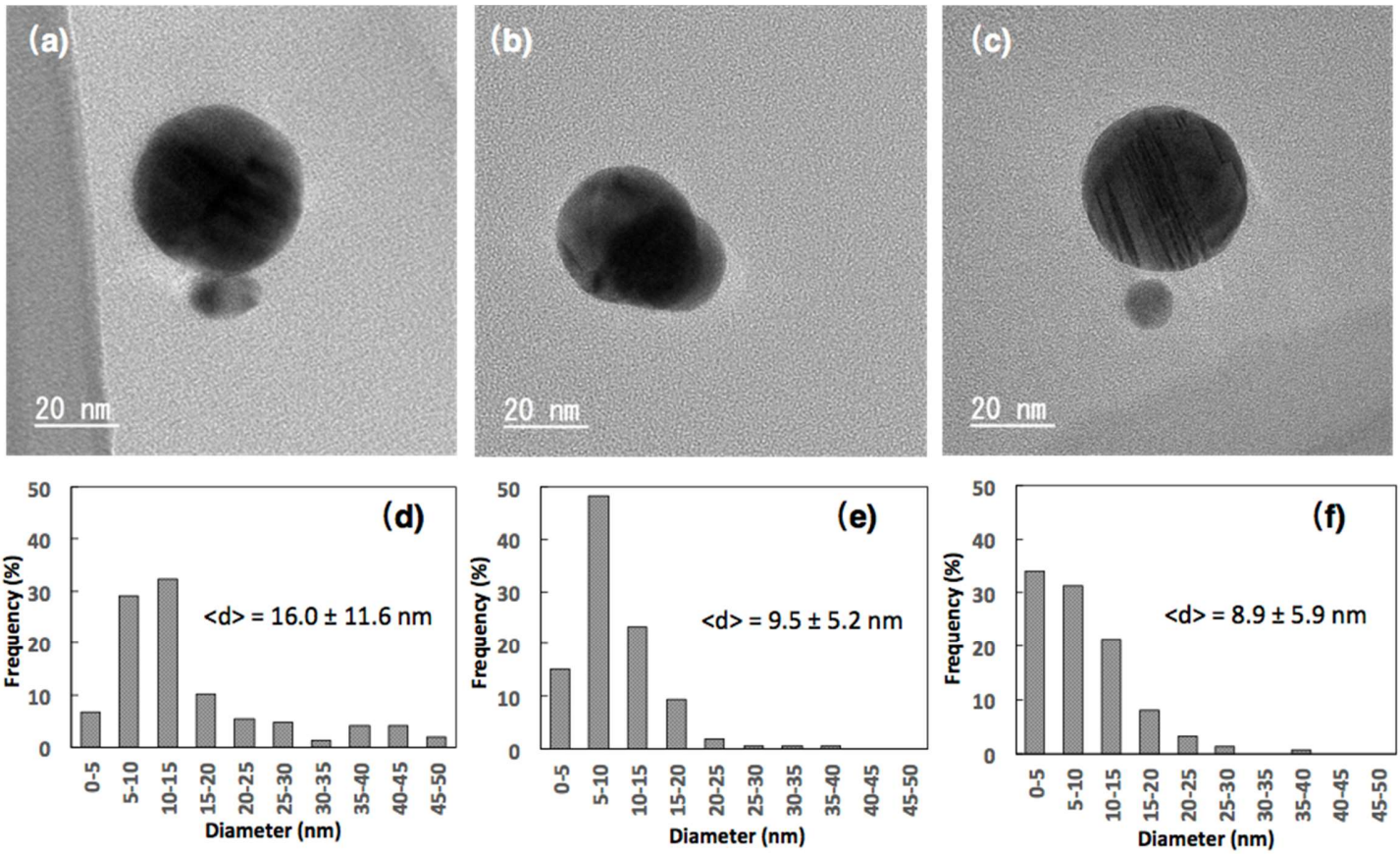

Figure 4. TEM images (top) and size distributions (bottom) of Au nanoparticles generated by PLA at CO_2 densities of (a), (d) 0.75 g/cm^3 (7.3 MPa; 23.4°C), (b), (e) 0.80 g/cm^3 (9.1 MPa; 24.5°C), and (c), (f) 0.89 g/cm^3 (17.5 MPa; 25.1°C).

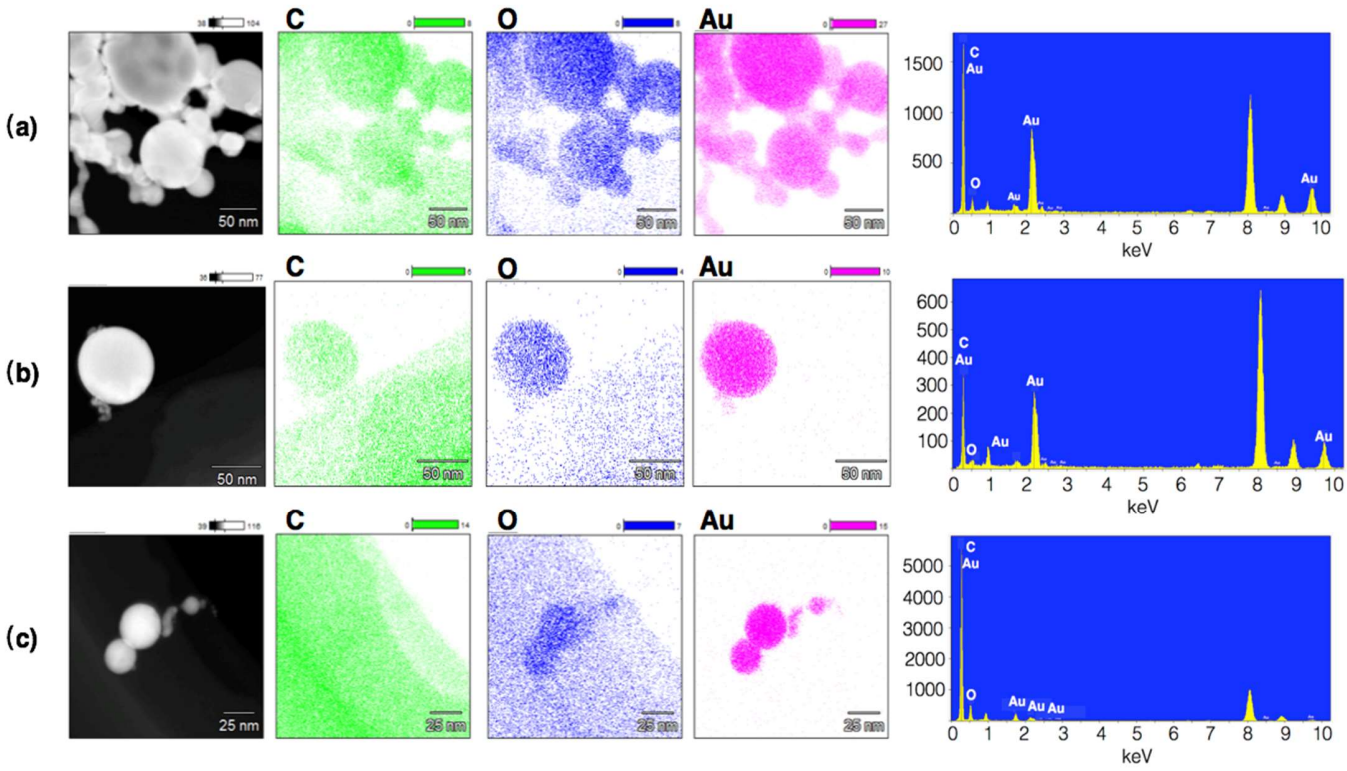

Figure 5. EDS mappings of particles generated at CO_2 densities of (a) 0.75 g/cm^3, (b) 0.80 g/cm^3, and (c) 0.89 g/cm^3.

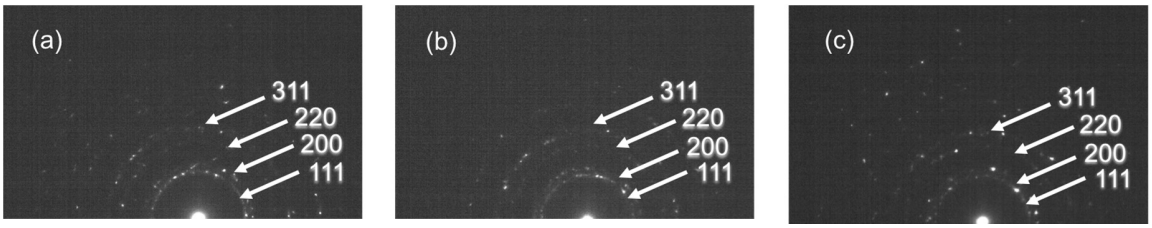

Figure 6. Electron diffraction pattern of particles generated at CO_2 densities of (a) 0.75 g/cm^3, (b) 0.80 g/cm^3, and (c) 0.89 g/cm^3.